JOURNAL OF MATERIALS SCIENCE 22 (1987) 4267–4273

Sialon formation by Si^+ and N_2^+ ion implantation into sapphire

SHOJI NODA, HARUO DOI, TATSUMI HIOKI, JUN-ICHI KAWAMOTO, OSAMI KAMIGAITO
Toyota Central Research and Development Laboratories, Inc., Nagakute-cho, Aichi-gun, Aichi-ken, 480-11 Japan

Single-crystal alumina was implanted firstly with 400 keV Si^+ and subsequently with N_2^+ ions and then annealed at 1673 K in an N_2 atmosphere. The implanted layers were characterized by means of X-ray diffraction, Rutherford backscattering–channelling of 2 MeV He^+ ions, and the resonance nuclear reaction $^{15}N(p, \alpha\gamma)^{12}C$. The annealing of sapphire implanted at ambient temperature resulted in the formation of β'-sialon, a solid solution of β-silicon nitride and alumina in the subsurface layer, while implantation at ~100 K resulted in the formation of aluminium oxynitride in the surface layer. In the latter case, the implanted silicon atoms were believed not to react with the implanted nitrogen atoms but with the substrate oxygen atoms. These crystalline precipitates were found to have epitaxial relations with the sapphire substrate.

1. Introduction

Ion implantation of ceramics has been demonstrated to significantly improve their mechanical properties [1–8] in an as-implanted state as well as after a post-implantation annealing. In an as-implanted state, a thin compressive surface layer and a thin amorphous soft surface layer in the substrate ceramic have been shown to be effective for obtaining improvements. A post-implantation annealing provides a variety of surface layers on the substrate ceramic. It has been reported that precipitates (metal or oxide) are embedded in an ion-implanted subsurface layer or they are formed on the top surface of the substrate [1, 6, 8–13] and that a ceramic alloy is also formed in the substrate layer of Cr^+-ion implanted alumina [10, 11]. These surface layers have been shown to bring about improvements in the mechanical properties. In the present work, we studied the microstructural modification of a single-crystal alumina surface by Si^+ and N_2^+ ion implantations, followed by a thermal annealing. There has been a little work on thermal annealing effects in ceramics implanted with multiple ions [13]. The implantation of multiple ions, followed by an adequate thermal annealing, may expand the possibilities of creating new materials on the substrate surface.

2. Experimental procedure

Single-crystal alumina plates (5 mm × 20 mm × 1 mm), whose major surfaces were normal to the ⟨0 0 0 1⟩ crystal axis, were used as substrates. Hereafter, single-crystal alumina is described as sapphire. One of the major surfaces was polished to a mirror finish and then the substrates were annealed at 1773 K in air for 5 h to remove residual stresses due to the surface finish. This thermal annealing was important to make the Rutherford backscattering (RBS)–channelling experiments successful. The polished surface was implanted firstly with 400 keV $^{28}Si^+$ and subsequently with 400 keV $^{14}N_2^+$ ions from a 400 kV Cockcroft–Walton type of ion implanter at ambient temperature or at about 100 K. For low-temperature implantation, the substrate was set on a copper holder containing liquid N_2. A small part of the substrate surface was masked to remain unimplanted and the ion beam was slightly tilted from the normal axis of the substrate to avoid ion-channelling. The projected ranges (R_p) of the 400 keV Si^+ and 400 keV N_2^+ ions in alumina are 288 and 280 nm, respectively, according to the Lindhand–Scharff–Schiott (LSS) theory [14]. The Si^+ ions were firstly implanted into the substrate to a given dose and then the N_2^+ ions were implanted to a dose smaller by about 30% than the Si^+ ion dose. Occasionally, $^{15}N_2^+$ ions were implanted to determine the depth distribution of the implanted nitrogen atoms by means of the resonance nuclear reaction, $^{15}N(p, \alpha\gamma)^{12}C$. The ion-implanted substrates were annealed at a temperature from 1473 to 1723 K in an N_2-flow alumina tube for 2 h. RBS–channelling experiments with a 2 MeV He^+ ion beam were carried out to characterize the ion-implanted layer before and after the thermal annealing. X-ray diffraction experiments were also done to determine the new phases generated by the ion implantation and the post-implantation annealing.

3. Results and discussion

3.1. X-ray diffraction analysis of implanted sapphire

X-ray diffraction spectra of sapphire, implanted at ambient temperature firstly with 400 keV Si^+ and subsequently with 400 keV N_2^+ ions whose doses were 2×10^{17} Si^+ cm^{-2} and 1.4×10^{17} N_2^+ cm^{-2}, are shown in Fig. 1a. The Co$K\alpha$ line ($\lambda = 0.17902$ nm) was used for the X-ray diffraction experiments. In the as-

0022–2461/87 $03.00 + .12

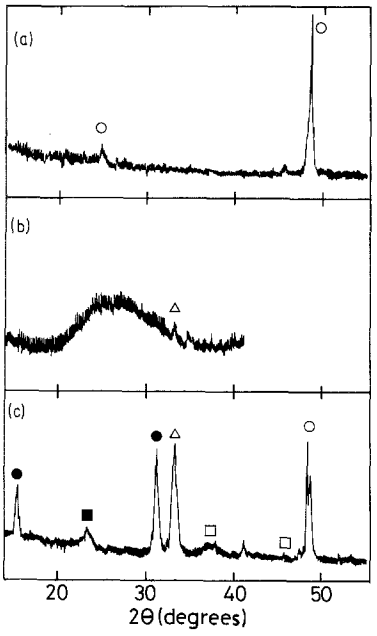

Figure 1 X-ray diffraction spectra of sapphire implanted at ambient temperature with 400 keV Si^+ and 400 keV N_2^+ ions to doses of 2×10^{17} Si^+ cm^{-2} and 1.4×10^{17} N_2^+ cm^{-2}; (○) alumina, (●) β'-sialon, (△) silicon, (□) 15R sialon, (■) unidentified. (a) As-implanted state, (b) annealed in N_2 at 1473 K, (c) annealed in N_2 at 1673 K.

implanted sapphire, only the diffraction lines assigned to alumina ((0 0 3) and (0 0 6) planes) are detected as shown in Fig. 1a. After annealing the implanted sapphire at 1473 K, a very weak signal assigned to the silicon (1 1 1) plane and a broad signal with a maximum at $2\theta \sim 25°$ are observed as shown in Fig. 1b. The broad signal is not identified yet. The annealing at 1673 K resulted in some distinctive diffraction lines other than the line due to alumina. The diffraction at $2\theta = 33.3°$ is assigned to the silicon (1 1 1) plane and the lines at $2\theta = 15.5°$ and 31.3° to the β'-sialon (1 0 0) and (2 0 0) planes. β'-sialon is a solid solution of α-alumina and β-silicon nitride [15–18]. The lines at 37.8 and 46° are tentatively

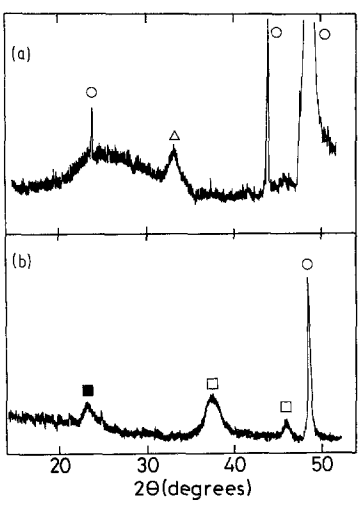

Figure 2 X-ray diffraction spectra of sapphire implanted at ambient temperature with 400 keV Si^+ and 400 keV N_2^+ ions to doses of 1×10^{17} Si^+ cm^{-2} and 7×10^{16} N_2^+ cm^{-2}; (○) alumina, (△) silicon, (□) 15R sialon, (■) unidentified. (a) Annealed in N_2 at 1473 K, (b) annealed in N_2 at 1673 K.

assigned to the 15R-sialon (0 0 1 5) and (0 0 1 8) planes. 15R-sialon is a polytype of aluminium nitride and has a hexagonal structure [17]. The reported lattice constant c is 4.18 nm and the observed one is 4.14 nm. The line at $2\theta = 23.3°$ remains unidentified. Fig. 2 is the X-ray diffraction spectrum of sapphire implanted with Si^+ and N_2^+ ions to doses of 1×10^{17} Si^+ cm^{-2} and 7×10^{16} N_2^+ cm^{-2} and annealed at 1473 or 1673 K. Upon annealing at 1473 K the implanted sapphire gives a diffraction spectrum consisting of the silicon (1 1 1) line, alumina (0 0 3) and (0 0 6) lines and the unidentified broad line as shown in Fig. 2a. The sharp line at 44.0° is the alumina (0 0 6) diffraction line of Co$K\beta$ X-rays. In ion-implanted sapphire after annealing at 1673 K, the lines tentatively assigned to 15 R-sialon are observed with the unidentified line at $2\theta = 23.3°$ and the alumina (0 0 6) line as shown in Fig. 2b. It is noted that β'-sialon was not formed by the 1673 K annealing of sapphire implanted with Si^+ and N_2^+ ions to the lower doses.

The β'-sialon unit cell is like that of β-silicon nitride, i.e. hexagonal, and has a range of homogeneity

$$Si_{6-x}Al_xO_xN_{8-x}$$

extending along the join Si_3N_4–$\frac{4}{3}(Al_2O_3)(AlN)$ from $x = 0$ to about $x = 4$ in the system Si_3N_4–$(AlN)_4$–$(Al_2O_3)_2$–$(SiO_2)_3$ [17]. The lattice constants a and c are found experimentally to be proportional to the alumina content [16, 18]. With the experimental lattice constant a of 0.766 nm, the relation between a and the alumina content leads to the result that β'-sialon contains about 34 wt % Al_2O_3 or the x value is about 1.7 in the above formula. X-ray diffraction analysis also showed that the β'-sialon is formed in such a manner that the (1 0 0) plane becomes parallel to the basal plane of α-alumina. Other precipitates are also formed in specified crystallographic relations to the substrate crystal: Si(1 1 1)//α-Al_2O_3 (0 0 0 1) and 15R-sialon (0 0 1)//α-Al_2O_3 (0 0 0 1). In sapphire implanted with Si^+ and N_2^+ ions to doses of 5×10^{16} Si^+ cm^{-2} and 5×10^{16} N_2^+ cm^{-2}, no diffraction line other than those of α-alumina was detected even after annealing at 1673 K. The intensity of the diffraction line due to a precipitate may be too small to detect by a conventional X-ray diffractometer.

In sapphire implanted at low temperature with Si^+ and N_2^+ ions, compounds different from those aforementioned are found to be formed by the thermal annealing. Fig. 3 is the X-ray diffraction spectrum of sapphire implanted at ~100 K firstly with Si^+ and subsequently with N_2^+ ions to doses of 2×10^{17} Si cm^{-2} and 1.4×10^{17} N_2^+ cm^{-2}, and then annealed at 1573 K. In addition to the diffraction lines ascribed to α-alumina, diffraction lines at $2\theta = 22.7$ and 46.3° are clearly observed. These lines may be assigned to the (1 1 1) and (2 2 2) planes of aluminium oxynitride (ALON), which is of a spinel structure. Another possibility is γ-alumina, which is also of a spinel structure. γ-Alumina is known to be generated when amorphous alumina crystallizes at temperature below 1273 K, but it is reported to change to α-alumina at temperatures above 1273 K [19]. Very weak diffraction lines due to mullite, $3Al_2O_3 \cdot 2SiO_2$, are also found in

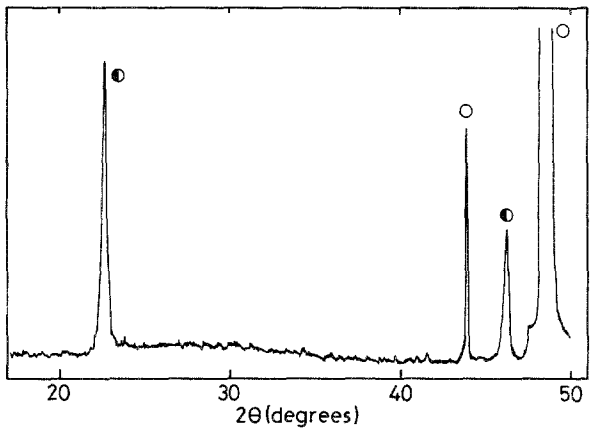

Figure 3 X-ray diffraction spectrum of sapphire implanted at ambient temperature with 400 keV Si^+ and 400 keV N_2^+ ions to doses of 2×10^{17} Si^+ cm^{-2} and 1.4×10^{17} N_2^+ cm^{-2}, and annealed in N_2 at 1573 K; (○) alumina, (◐) aluminium oxynitride.

Fig. 3. The annealing at 1673 K made the ALON lines weaker but the mullite lines slightly stronger. After the annealing at 1723 K, apart from substrate alumina lines only weak mullite lines were detected by X-ray diffraction analysis.

Aluminium oxynitride is of the general formula

$$Al_{8/3+x/3}O_{4-x}N_x$$

where x, the number of oxygens replaced by nitrogen, ranges from 0.22 to 0.50 [20]. From the reported relation between the lattice constant and x, and the observed lattice constant, 7.9, the value of x is found to be 0.22. In sapphire implanted at ~ 100 K with Si^+ and N_2^+ ions and annealed at 1573 K, aluminium oxynitride with $x \simeq 0.22$ is formed in such a manner that the (1 1 1) plane becomes parallel to the (0 0 0 1) plane of α-alumina.

3.2. RBS–channelling analysis of implanted sapphire

Fig. 4 is the RBS–channelling spectrum of sapphire implanted at ambient temperature with Si^+ and N_2^+ ions to doses of 2×10^{17} Si^+ cm^{-2} and 1.4×10^{17} N_2^+ cm^{-2} and subsequently annealed at 1473 K. The channelling spectrum was obtained with 2 MeV He^+ probe ions parallel to the ⟨0 0 0 1⟩ axis of sapphire. It is evident from Fig. 4 that silicon atoms do not exist in any form on the top surface of sapphire and that the implanted region is completely random, but the surface region to a depth of about 150 nm is almost perfectly crystalline.

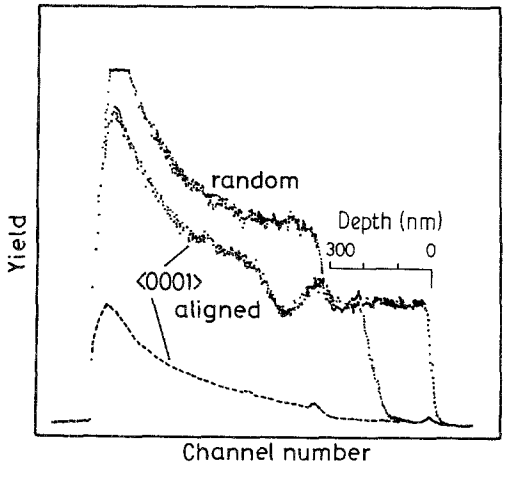

Figure 4 RBS–channelling spectra of sapphire implanted at ambient temperature with 400 keV Si^+ and N_2^+ ions to doses of 2×10^{17} Si^+ cm^{-2} and 1.4×10^{17} N_2^+ cm^{-2} and annealed at 1473 K in N_2. The channelling spectrum (– – –) of unimplanted sapphire is also shown in the figure.

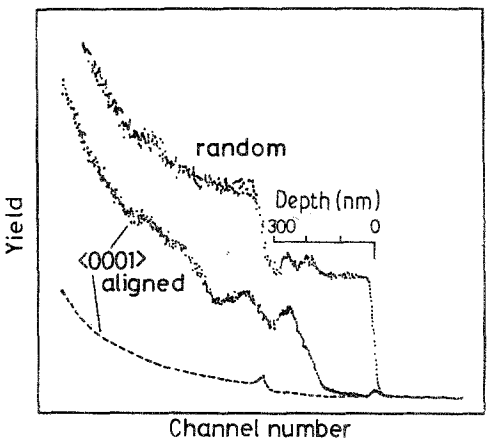

Figure 5 RBS–channelling spectra of sapphire implanted at ambient temperature with 400 keV Si^+ and N_2^+ ions to doses of 2×10^{17} Si^+ cm^{-2} and 1.4×10^{17} N_2^+ cm^{-2} and annealed at 1673 K in N_2. The channelling spectrum (– – –) of unimplanted sapphire is also shown in the figure.

For sapphire implanted at ambient temperature with Si^+ and N_2^+ ions to doses of 2×10^{17} Si^+ cm^{-2} and 1.4×10^{17} N_2^+ cm^{-2} and annealed at 1673 K, the RBS–channelling spectrum is shown in Fig. 5. In this specimen, β′-sialon is formed in such a manner that the (1 0 0) plane becomes parallel to the (0 0 0 1) plane of sapphire as mentioned in the preceding section. The surface region shows almost perfect crystalline order and the crystalline order of the implanted region also recovers rather well. We tried to analyse the RBS random spectrum shown in Fig. 5 by a computer simulation technique [21] in order to get more probable concentration depth profiles of the elements. In the simulation, the depth profile of ^{15}N atoms was employed, this being determined by means of the resonance nuclear reaction $^{15}N(p, \alpha\gamma)^{12}C$ as described later. The observed spectrum was rather satisfactorily simulated as shown in Fig. 6a, except for a slightly smaller backscattering yield from the aluminium sublattice in the observed spectrum. This implies that the observed spectrum was not a perfectly random spectrum.

The concentration depth profiles of the elements deduced from the simulation are also shown in Fig. 6b. To convert the depth scale from the unit of atoms cm^{-2} to that of nanometres, the atom density of pure alumina (1.165×10^{23} atoms cm^{-3}) was employed. From the concentration depth profiles shown in Fig. 6b and the X-ray diffraction results, it is inferred that β′-sialon exists in a subsurface layer just beneath the crystalline alumina surface layer and that crystalline silicon exists beneath the β′-sialon layer. The composition ratio of the crystalline silicon–alumina composite layer may also imply that some implanted silicon atoms combine with matrix oxygens. The RBS–channelling spectrum shown in Fig. 5 suggests that the crystalline

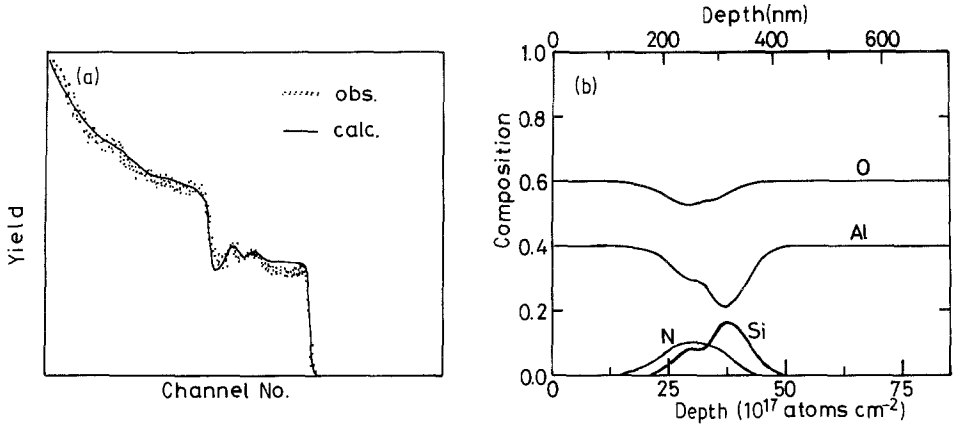

Figure 6 (a) Computer simulation analysis of the RBS random spectrum given in Fig. 5; (· · ·) observed, (——) calculated. (b) Depth profiles of the elements deduced from the simulation.

array of the β'-sialon layer has a good coherency to that of sapphire matrix. In sapphire implanted at ambient temperature, the implanted atoms are trapped in the subsurface region and the surface layer of about 150 nm thickness is an almost perfect α-alumina crystal after annealing at 1673 K.

It is known that the surface layer becomes amorphous at a dose as low as $\sim 2 \times 10^{15}$ ions cm^{-2} when sapphire is ion-implanted at a low temperature [2, 13, 22]. The threshold dose for surface amorphization depends on the mass and energy of the incident ions; for a given incident ion a larger dose is required to make the surface layer amorphous in case the incident ions have a larger energy. Annealing the implanted sapphire whose surface becomes amorphous, the implanted atoms are forced to move up to the surface because of the epitaxial forward regrowth of the amorphous alumina to the surface from the deep undamaged crystal region [11]. Microhardness has been shown to be a good index of the surface amorphization induced by ion implantation [2, 13]. The Knoop microhardness (normal load: 0.24 N) was found to be ~ 16 GPa for a sapphire surface implanted at ~ 100 K with Si^+ and N_2^+ to doses of 2×10^{17} Si^+ cm^{-2} and 1.4×10^{17} N_2^+ cm^{-2}, and it is about half that for the unimplanted sapphire surface.

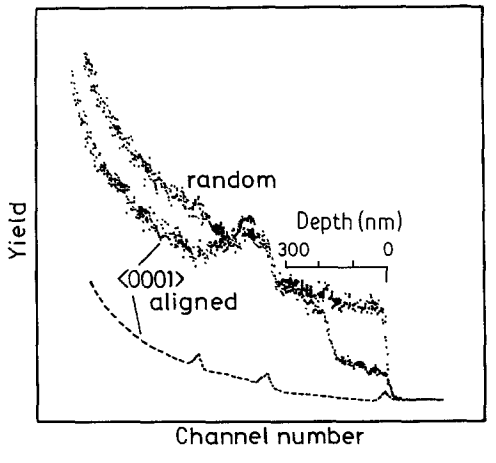

Figure 7 The RBS–channelling spectra of sapphire implanted at ~ 100 K with 400 keV Si^+ and 400 keV N_2^+ ions to doses of 2×10^{17} Si^+ cm^{-2} and 1.4×10^{17} N_2^+ cm^{-2} and annealed at 1573 K in N_2. The channelling spectrum (– – –) of unimplanted sapphire is also shown in the figure.

This suggests that the surface layer implanted at a low temperature becomes amorphous.

Fig. 7 shown the RBS–channelling spectra of sapphire implanted at ~ 100 K with Si^+ and N_2^+ to doses of 2×10^{17} Si^+ cm^{-2} and 1.4×10^{17} N_2^+ cm^{-2} and annealed at 1573 K. In this specimen, aluminium oxynitride and a small amount of mullite are formed as described in the preceding section. A simulation analysis of the random spectrum given in Fig. 7 was also carried out, and the results are given in Fig. 8 together with the concentration depth profiles deduced from the simulation. These concentration profiles imply that the surface layer of about 200 nm thickness is aluminium oxynitride and that silicon atoms exist rather uniformly in a subsurface layer of about 290 nm thickness beneath the aluminium oxynitride surface layer. The crystalline order of the surface layer is partially recovered but the implanted subsurface region remains random after annealing at 1573 K.

Fig. 9 is the RBS–channelling spectra of sapphire implanted at ~ 100 K with Si^+ and N_2^+ to doses of 2×10^{17} Si^+ cm^{-2} and 1.4×10^{17} N_2^+ cm^{-2} and annealed at 1723 K. From the random spectrum it may be deduced that the silicon atoms are still embedded in the subsurface layer while the nitrogen atoms are released from the surface. The crystalline order of the implanted subsurface layer is still random and that of the surface layer is only partially recovered. It is interesting to note that outward diffusion of the implanted silicon atoms to the surface did not occur upon annealing the sapphire implanted at ~ 100 K, whose surface layer was confirmed to be amorphous by the microhardness measurement.

As to the crystalline recovery of the implanted subsurface and surface layers, a big difference is found between sapphires implanted with Si^+ and N_2^+ at ambient temperature and at ~ 100 K. In sapphire implanted at a low temperature, an Si–Al–O subsurface layer may be stable and block forward epitaxial crystal regrowth from the unimplanted substrate layer, and very few or no crystal seeds may be available to regrow crystalline alumina in the surface layer. It is well known that amorphous alumina transforms to γ-alumina (spinel structure) at a temperature around 1273 K. On the way to the transformation, nitrogen atoms may be incorporated into the lattice sites and

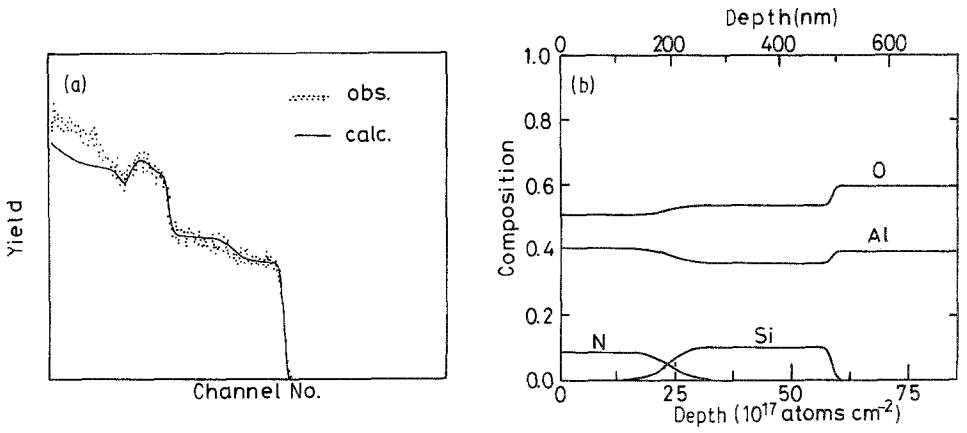

Figure 8 (a) Computer simulation analysis of the RBS random spectrum given in Fig. 7; (···) observed, (——) calculated. (b) Depth profiles of the elements deduced from the simulation.

then an aluminium oxynitride of spinel type is thought to be formed instead of γ-alumina. It is also interesting to note that silicon crystals are formed in sapphire implanted at ambient temperature but not in sapphire implanted at low temperature. This is also consistent with the fact that the Si–Al–O subsurface layer, which may be an amorphous phase, is stable in the relevant circumstances.

3.3. Depth profile of the implanted nitrogen atoms by the resonance nuclear reaction $^{15}N(p, \alpha\ \gamma)^{12}C$

The RBS method is in general a powerful means to study the structure of an ion-implanted layer, but it gives only limited information in cases where the mass number of the implanted ion is nearly equal to or smaller than that of any target atom. The implantation of Si^+ and N_2^+ ions into alumina is such a case. In such circumstances, a high-energy ion-beam analysis is still quite useful if a suitable resonance nuclear reaction is available. There is a resonance nuclear reaction, $^{15}N(p, \alpha\ \gamma)^{12}C$, for one of the isotopes of the nitrogen atom. One of the resonance energies is 889 keV and its width is 2.2 keV [23]. Fig. 10 is the depth profile of ^{15}N atoms in sapphire implanted at ambient temperature with Si^+ and $^{15}N_2^+$ to doses of 2×10^{17} Si^+ cm^{-2} and 1.4×10^{17} N_2^+ cm^{-2} and annealed at 1673 K. This depth profile was determined by measuring the yield of the emitted γ-rays (4.43 MeV) as the incident proton energies increased successively by about 2 keV from 898 keV. The depth distribution of the implanted ^{15}N atoms is nearly Gaussian even after annealing at 1673 K, as shown in Fig. 10. The depth for the maximum concentration is about 270 nm and the width of the distribution for half the maximum concentration is about 155 nm, or the standard deviation of the Gaussian distribution is 66 nm. According to the LSS theory [14], the projected range R_p of 400 keV N_2^+ or 200 keV N^+ in alumina is about 280 nm and the standard deviation ΔR_p is about 52 nm. The depth profile of the implanted nitrogen atoms observed after annealing is found to be very similar to that calculated for the as-implanted state.

To evaluate the number of implanted nitrogen atoms remaining after the annealing, a silicon wafer implanted with 400 keV $^{15}N_2^+$ ions to a dose of 1×10^{16} N_2^+ cm^{-2} was used as a reference. By comparing the integrated yield of the γ-rays emitted from sapphire implanted with Si^+ and $^{15}N_2^+$ ions and annealed at 1673 K with that from the reference sample, it was found that about 43% of the implanted nitrogens, or 1.2×10^{17} N cm^{-2}, remained in the sapphire after the annealing. More than half the implanted nitrogens

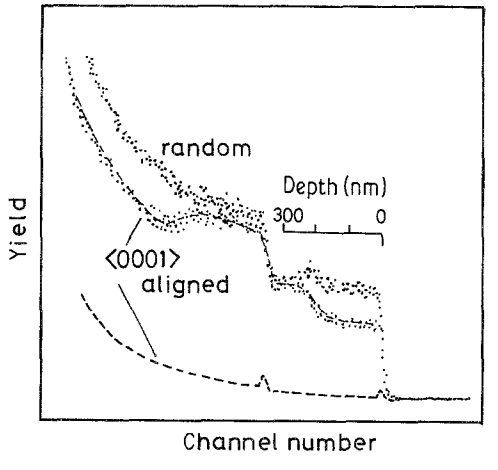

Figure 9 The RBS–channelling spectra of sapphire implanted at ~100 K with 400 keV Si^+ and 400 keV N_2^+ ions to doses of 2×10^{17} Si^+ cm^{-2} and 1.4×10^{17} N_2^+ cm^{-2} and annealed at 1723 K in N_2. The channelling spectrum (– – –) of unimplanted sapphire is also shown in the figure.

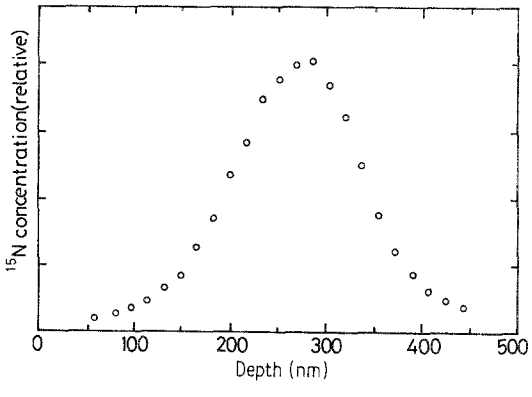

Figure 10 The depth profile of implanted ^{15}N atoms in sapphire implanted at ambient temperature with 400 keV Si^+ and 400 keV $^{15}N_2^+$ ions to doses of 2×10^{17} Si^+ cm^{-2} and 1.4×10^{17} N_2^+ cm^{-2} and annealed at 1673 K in N_2.

were freed from the implanted layer during the post-implantation annealing. Blisters with a diameter of about 10 μm were observed on the surface, which implies the bursting of nitrogen gas bubbles. The depth profile of the implanted ^{15}N atoms is nearly Gaussian as already mentioned. The maximum nitrogen concentration is evaluated to be 7.3×10^{21} N cm^{-3} ($\simeq N_T/2.5\Delta R_p$; $N_T = 1.2 \times 10^{17}$ N cm^{-2} and $\Delta R_p = 66$ nm where N_T is the total number of nitrogen atoms) at a depth of 270 nm from the surface.

4. Compound formation by post-implantation annealing: effect of implantation temperature

It is known that the implantation of a large number of nitrogen ions (an order of 10^{18} N^+ cm^{-2}) into a silicon wafer and adequate thermal treatment causes the formation of a buried insulating layer of silicon nitride in the silicon surface layer [24, 25]. In sapphire implanted with Si^+ and N_2^+ ions at ambient temperature, β'-sialon or a solid solution of β-silicon nitride and α-alumina is found to be formed in the subsurface layer. The relative densities of atoms in the implanted layer are evaluated to be Si : Al : O : N = 7.8 : 29.1 : 53.4 : 9.7 at the position where the nitrogen concentration is maximum as shown in Fig. 6b. On the other hand, the ratio of the constituent atoms of β'-sialon, $Si_{4.2}Al_{1.8}O_{1.8}N_{6.2}$, is Si : Al : O : N = 30.2 : 12.6 : 12.6 : 44.6. Supposing that all the nitrogen atoms remaining are used for β'-sialon formation, at most 10% of the alumina in a thin alumina slab is involved in β'-sialon formation. This estimation and the X-ray diffraction studies may mean that islands of β'-sialon occur in the sapphire subsurface and the (1 0 0) plane of β'-sialon is parallel to the basal plane of α-alumina. This speculation that β'-sialon is formed as islands seems to be consistent with the fact that we could not find any good fit of the RBS spectrum with the assumption of a buried homogeneous layer of β'-sialon. 15R-Sialon seems to be also formed as an island in a subsurface layer of sapphire.

About 50% of the implanted silicon atoms also precipitate as silicon microcrystals in the subsurface layer beneath the β'-sialon–alumina composite layer, and the (1 1 1) plane is parallel to the basal plane of α-alumina. Nearly half the amounts of implanted silicon and nitrogen atoms are used for β'-sialon formation. Nevertheless, β'-sialon was not formed in sapphire implanted with Si^+ and N_2^+ ions to doses of 1×10^{17} Si^+ cm^{-2} and 7×10^{16} N_2^+ cm^{-2} and annealed at 1673 K, but another compound was formed which is tentatively assigned to 15R-sialon. This suggests that the local concentrations of atoms where the embryo of a compound is generated determine the kind of compound formed by post-implantation annealing. In sapphire implanted firstly with Si^+ and subsequently with N_2^+ ions at $\sim$100 K, silicon atoms seem not to react with nitrogen atoms at 1573 and 1723 K. The atoms implanted at a low temperature are expected to disperse more or less "atomistically", while those implanted at ambient temperature or a temperature higher than room temperature generally coalesce to particles. It is probable that silicon atoms can react with nitrogen to produce embryoic silicon nitride when nitrogen ions are implanted into silicon particles embedded in the sapphire subsurface layer. In the atomistically dispersed state of silicon, aluminium, oxygen and nitrogen atoms, a silicon atom is expected to be more likely to bond to an oxgyen atom than to a nitrogen atom.

5. Summary

Islands of β'-sialon are suggested to be formed in the subsurface of a sapphire substrate when the substrate is implanted firstly with Si^+ and subsequently with N_2^+ ions at ambient temperature and then annealed at 1673 K in an N_2 atmosphere. β'-Sialon grows in such a manner that the (1 0 0) plane is parallel to the basal plane of α-alumina. On the other hand, aluminium oxynitride is formed in the surface layer of the substrate when the substrate is implanted with Si^+ and N_2^+ ions at $\sim$100 K and then annealed at 1573 K in an N_2 atmosphere. Aluminium oxynitride also grows in such a manner that the (1 1 1) plane is parallel to the basal plane of α-alumina. In the latter case the implanted silicon atoms are suggested not to react with the implanted nitrogen atoms but with oxygen atoms in the substrate. Silicon atoms implanted at ambient temperature are expected to aggregate to small particles, while those implanted at $\sim$100 K will disperse more or less atomistically. Some of the nitrogen atoms with which the substrate is bombarded after Si^+ implantation may impinge directly into small silicon particles embedded in the sapphire subsurface, and may react with the silicon atoms at a high temperature.

Acknowledgements

We would like to thank Dr Y. Kido for the measurement of the depth profile of ^{15}N atoms and for helpful discussion. We also appreciate Mr A. Itoh and Mr M. Ohkubo for their technical support.

References

1. T. HIOKI, A. ITOH, S. NODA, H. DOI, J. KAWAMOTO and O. KAMIGAITO, *Nucl. Instrum. Meth. Phys. Res.* **B7/8** (1985) 521.
2. T. HIOKI, A. ITOH, M. OHKUBO, S. NODA, H. DOI, J. KAWAMOTO and O. KAMIGAITO, *J. Mater. Sci.* **21** (1986) 1321.
3. P. J. BURNETT and T. F. PAGE, *ibid.* **19** (1984) 3524.
4. *Idem, ibid.* **20** (1985) 4624.
5. C. S. YUST and C. J. McHARGUE, *Mater. Sci. Res.* **17** (1984) 533.
6. H. NARAMOTO, C. J. McHARGUE, C. W. WHITE, J. M. WILLIAMS, O. W. HOLLAND, M. M. ABRAHAM and B. R. APPLETON, *Nucl. Instrum. Meth.* **209/210** (1983) 1159.
7. B. R. APPLETON, H. NARAMOTO, C. W. WHITE, O. W. HOLLAND, C. J. McHARGUE, G. FARLOW, J. NARAYAN and J. M. WILLIAMS, *Nucl. Instrum. Meth. Phys. Res.* **B1** (1984) 167.
8. K. O. LEGG, J. K. COCHRAN Jr, H. F. SOLNICK-LEGG and X. L. MANN, *ibid.* **B7/8** (1985) 535.
9. G. C. FARLOW, C. W. WHITE, C. J. McHARGUE, P. S. SKLAD and B. R. APPLETON, *ibid.* **B7/8** (1985) 541.
10. H. NARAMOTO, C. W. WHITE, J. M. WILLIAMS, C. J. McHARGUE, O. W. HOLLAND, M. M. ABRAHAM and B. R. APPLETON, *J. Appl. Phys.* **54** (1983) 683.

11. M. OHKUBO, T. HIOKI and J. KAWAMOTO, *ibid.* **60** (1986) 1325.
12. A. PEREZ, *Nucl. Instrum. Meth. Phys. Res.* **B1** (1984) 621.
13. C. W. WHITE, G. C. FARLOW, C. J. McHARGUE, P. S. SKLAD, M. P. ANGELINI and B. R. APPLETON, *ibid.* **B7/8** (1985) 473.
14. J. LINDHARD, M. SCHARFF and H. E. SCHIOTT, *Mat. Fys. Medd. Dan. Vid. Selsk.* **33** (1963) No. 14.
15. Y. OYAMA and O. KAMIGAITO, *Jpn J. Appl. Phys.* **10** (1971) 1637.
16. *Idem, Yogyo-Kyokai-Shi* **80** (1972) 327.
17. K. H. JACK, in "Nitrogen Ceramics", edited by F. L. Riley (Noordhoff, Leyden, 1977) pp. 109–128.
18. *Idem, Trans. J. Br. Ceram. Soc.* **72** (1973) 376.
19. R. KELLY, *Nucl. Instrum. Meth.* **182/183** (1981) 351.
20. JCPDS File No. 18-52 (International Centre for Diffraction Data, Pennsylvania, 1981).
21. Y. KIDO and J. KAWAMOTO, *J. Appl. Phys.* **61** (1987) 956.
22. C. J. McHARGUE, G. C. FARLOW, C. W. WHITE, J. M. WILLIAMS, B. R. APPLETON and H. NARAMOTO, *Mater. Sci. Eng.* **69** (1985) 123.
23. L. C. FELDMAN and S. T. PICRAUX, in "Ion Beam Handbook for Material Analysis", edited by J. W. Mayer and E. Rimini (Academic, New York, 1977) pp. 205–223.
24. P. BOURGUET, J. M. DUPART, E. Le TIRAN, P. AUVRAY, A. GUIVARC'H, M. SALVI, G. PELOUS and P. HENOC, *J. Appl. Phys.* **51** (1980) 6169.
25. T. TSUJIDE, M. NOJIRI and H. KITAGAWA, *ibid.* **51** (1980) 1605.

Received 10 November 1986
and accepted 29 May 1987